

A record of aerobic methane oxidation in tropical Africa over the last 2.5 Ma

Charlotte L. Spencer-Jones^a, Thomas Wagner^{b,a*}, Helen M. Talbot^a

^aSchool of Civil Engineering and Geosciences, Drummond Building, Newcastle University,
Newcastle upon Tyne, NE1 7RU, UK

^bLyell Centre, Heriot-Watt University, Edinburgh, EH14 4AP, UK

* Corresponding author. Tel.: +44 (0)131 451 3300; *E mail address*: t.wagner@hw.ac.uk (T. Wagner).

Charlotte L. Spencer-Jones^a, *now at*: Department of Geography, Durham University,
Durham, DH 1 3LE, UK.

Abstract

Methane and CO₂ are climatically active greenhouse gases (GHG) and are powerful drivers of rapid global warming. Comparable to the Arctic, the tropics store large volumes of labile sedimentary carbon that is vulnerable to climate change. However, little is known about this labile carbon reservoir, in particular the behaviour of high methane-producing environments (e.g. wetlands), and their role in driving or responding to past periods of global climate change. In this study, we use a microbial biomarker approach that traces continental aerobic methane oxidation (AMO) from sedimentary organic matter in deep-sea fan sediments off the Congo River to reconstruct the link between central African methane cycling and continental export during key periods of global Pleistocene warmth. We use 35-amino bacteriohopanepolyols (BHPs), specifically aminobacteriohopane-31,32,33,34-tetrol (aminotetrol) and 35-aminobacteriohopane-30,31,32,33,34-pentol (aminopentol) as diagnostic molecular markers for AMO (CH₄ oxidation markers) and the prevalence of continental wetland environments. BHPs were analysed in sediments from the Congo fan (ODP 1075) dated to 2.5 Ma. High resolution studies of key warm marine isotope stages (MIS) 5, 11 and 13 are included to test the relationship between CH₄ oxidation markers in sediments at different levels of elevated global atmospheric GHG.

This study presents the oldest reported occurrence, to date, of 35-amino BHPs up to 200 meters below sea floor (~2.5 Ma) with no strong degradation signature observed. Low concentrations of CH₄ oxidation markers identified between 1.7 Ma and 1 Ma suggest a reduction in wetland extent in tropical Africa in response to more arid environmental conditions. Correlation of high resolution CH₄ oxidation marker signatures with global atmospheric GHG concentrations during MIS 5, 11 and 13

further emphasize periods of enhanced tropical C cycling. However, subsequent analysis would be required to further extrapolate the relative importance of tropical methane sources as a driver of global methane concentrations during the Pleistocene.

Key words

Pleistocene, Congo, wetland, methane cycle, methanotrophic bacteria, bacteriohopanepolyols

1 1. INTRODUCTION

2 During the past century, Earth has experienced a rapid rise in surface temperature
3 with instrumental records showing the past 30 years to have been successively
4 warmer than the previous decades (IPCC, 2013). In parallel with this rise, significant
5 increase in the atmospheric concentrations of greenhouse gasses (GHG) have been
6 recorded, with methane (CH₄) and carbon dioxide (CO₂) being particularly potent
7 GHG and potential drivers of climate change (IPCC, 2013). Changes in atmospheric
8 temperatures and the hydrological cycle have a coupled impact on biogeochemical
9 cycles, including the C cycle. Perturbations in the C cycle could lead to the
10 degradation of vulnerable C sources such as wetlands (IPCC, 2013). While modern
11 elevated atmospheric GHG concentrations are of natural and anthropogenic origins,
12 the source of them in the palaeo-record as a climate and ecosystem regulator
13 remains unclear. Within the modern terrestrial system, wetlands are the largest
14 natural source of CH₄ and are estimated to account for ~70% of all natural emissions
15 (Wuebbles and Hayhoe, 2002) with tropical wetlands (20°N to 30°S) identified as the
16 largest CH₄ producers (Bartlett and Harriss, 1993; Sjogersten et al., 2014). Changes
17 in the extent and volume of tropical methane sources and sinks (i.e. wetlands and
18 atmospheric oxidation), modulated by fluctuations in the hydrological cycle and
19 vegetation feedbacks, have been shown to exert a significant control on atmospheric
20 methane concentrations over the past 800 ka (e.g. Blunier et al., 1995; Loulergue et
21 al., 2008; Singarayer et al., 2011).

22 Paleoclimate analysis of West African marine sedimentary archives suggests
23 significant variations in continental aridity and humidity during the Pleistocene
24 leading to the destabilisation of vegetation zones (Scheffuß et al., 2003). Biomarker
25 and pollen analysis of deep-sea sedimentary archives from North West Africa

26 reveals major changes in the balance between C₃ and C₄ vegetation, reflecting
27 significant changes in climate during the past 160 ka (Zhao et al., 2003).
28 Furthermore, biomarker and pollen analysis from southwest African margin
29 sediments along a transect of 9 sites from Congo (4°S) to Cape Bush (30°S) reveal
30 an expansion of C₄ plant indicators during Holocene glacial periods, thus indicating a
31 northward expansion of arid zones favouring grass vegetation (Rommerskirchen et
32 al., 2006). While the quantitative impact of habitat expansion on C cycling remains to
33 be resolved, the expansion of mangroves and wetland environments during these
34 warm periods may have resulted in an increased flux in CH₄ and other GHG to the
35 atmosphere. Indeed, ice core records suggest that changes in the strength of tropical
36 CH₄ reservoirs had an important control on the global atmospheric CH₄ budget
37 during the past 800 ka (Petit et al., 1999; Loulergue et al., 2008). However, direct
38 measurements of atmospheric CH₄ concentration beyond 800 ka are not available
39 from ice cores, requiring an independent proxy approach to explore CH₄ dynamics
40 further back in time, and in non-glacial environments. It has been shown that specific
41 biomarker records are powerful proxies for reconstructing C cycling beyond this time
42 period of direct measurements (Talbot et al., 2014).

43 Bacteriohopanepolyols (BHPs) are highly functionalised pentacyclic triterpenoids
44 produced by many aerobic as well as a number of obligate and facultative anaerobic
45 bacteria (e.g. Rohmer et al., 1984; Talbot et al., 2008; Eickhoff et al., 2013; and
46 references therein). Some BHPs with an amino group at the C-35 position (35-amino
47 BHPs) are thought to be specific indicators of aerobic methane oxidation (AMO) with
48 35-aminobacteriohopane-31,32,33,34-tetrol (aminotetrol; **II**; Table 1); 35-
49 aminobacteriohopane-30,31,32,33,34-pentol (aminopentol; **III**), unsaturated
50 aminopentol (**IV/V**) and aminopentol isomer (**III'**; van Winden et al., 2012b) being

51 almost exclusively produced by aerobic methanotrophs (Talbot and Farrimond, 2007;
52 Zhu et al., 2010; van Winden et al., 2012b; Berndmeyer et al., 2013; hereafter referred
53 to as CH₄ oxidation markers). CH₄ oxidation markers have been identified in both
54 terrestrial and marine settings, including but not limited to; peatlands (van Winden et
55 al., 2012a; 2012b; Talbot et al., 2016), a stratified post glacial lake in Antarctica
56 (Coolen et al., 2008), and within suspended particulate matter in ocean settings
57 (Blumenberg et al., 2007; Wakeham et al., 2007; Sáenz et al., 2011), modern soils
58 from the Amazon (Wagner et al., 2014) and Congo hinterland (Spencer-Jones et al.,
59 2015), and ancient sediments from the Amazon (Wagner et al., 2014) and Congo
60 (Talbot et al., 2014) fans. However, despite the variety of terrestrial and marine
61 environments where these biomarkers have been found, current research suggests
62 that when found in marine sediments they are primarily of terrestrial origin (Talbot et
63 al., 2014; Wagner et al., 2014; Schefuß et al., 2016), specifically from catchment
64 wetlands (Spencer-Jones et al., 2015). Large scale fluctuations in the concentration
65 of these compounds during warm – humid interglacial periods have been associated
66 with hydrological changes and corresponding fluctuations in wetland extent (Talbot
67 et al., 2014; Schefuß et al., 2016). Furthermore, hydrologically induced variations in
68 Congo wetland systems during the Holocene resulted in the export of pre-aged OM
69 during arid conditions and younger-OM during humid environmental conditions
70 (Schefuß et al., 2016) potentially leading to lags in biomarker export during past
71 glacial (dry) and at the transition to interglacial (humid) Termination conditions. A
72 previous low-resolution study was limited to the first ~1.2 Ma (115.65 meters below
73 sea floor, m.b.s.f) of a Congo deep-sea fan core (ODP 1075) and, therefore, could
74 not resolve some of the short term variability in 35-amino BHP distributions and,
75 thus, AMO cycling during the earlier parts of the Pleistocene (Talbot et al., 2014).

76 This study expands on previous research by addressing the causes and implications
77 of short- and long term variability in CH₄ oxidation markers in the Congo fan record
78 (Talbot et al., 2014). This study also explores the fluctuations in CH₄ oxidation
79 markers under different, elevated atmospheric GHG concentrations. We first test the
80 stratigraphic suitability of 35-amino BHPs for palaeoclimate reconstructions in ODP
81 1075 sediments by expanding the record to the core's maximum depth of 201.25
82 m.b.s.f (~2.5 Ma). Building on this assessment, we introduce high resolution records
83 of CH₄ oxidation marker concentration for marine isotope stages (MIS) 2-6 and 10-
84 13 to address changes in short term variability in terrestrial CH₄ cycling. These
85 intervals include MIS 5 and 11, which are both considered particularly warm stages
86 in the geologic record with approximate durations of 58 ka and 64 ka, respectively
87 (Howard, 1997; Kukla et al., 1997; Spahni et al., 2005). MIS 5 and 11 are
88 characterised as periods of reduced ice volume with an interglacial and multiple
89 interstadials and stadials (Loutre et al., 2003) and may serve as potential analogues
90 for Earth's future climate. BHP distributions of MIS 5 and 11 are contrasted with the
91 intermediate warm period MIS 13 and cool MIS 2, 3, 4, 6, 10, and 12, to further test
92 the sensitivity of the biomarkers to global GHG levels and improve characterisation
93 of short-term transitions in AMO variation during the Pleistocene.

94 **2. MATERIALS AND METHODS**

95 **2.1. SITE LOCATION AND SAMPLE DESCRIPTION**

96 The Congo River is the largest river in Africa and the second largest river in the
97 world in terms of drainage basin size (~3.7 x 10⁶ Km²; Runge, 2007; Laraque et al.,
98 2009) and supplies freshwater, nutrients (including large amounts of SiO₂) and
99 sediment to the ocean. The Congo River plume extends 800 Km offshore and can be

100 detected during austral summer when monsoon/precipitation reach their maximum
101 seasonal intensity (Anka and Séranne, 2004). The rapid outflow of the Congo River
102 is caused by the relatively small river mouth and a large canyon head (Berger et al.,
103 2002). As a result of coastal, oceanic and river induced upwelling, modern primary
104 production is very high in the surface waters off the Congo continental margin (Anka
105 and Séranne, 2004).

106 Sedimentation within the Congo fan is dominated by rainout of suspended clays
107 derived from the Congo River and by pelagic settling of biogenic debris (Berger et
108 al., 2002). The lower Congo basin sediments lack a significant river borne sand and
109 silt fraction, due to most of the coarse debris being deposited before it reaches the
110 ocean (Spencer et al., 2012).

111 The Congo catchment hosts extensive wetland and water dependent ecosystems
112 and supports one of the world's largest swamp forests (360 000 Km²; Bwangoy et
113 al., 2010). One prominent example is Malebo Pool, located on the main stem of the
114 Congo River (Fig. 1). Organic matter (OM) exported from this region has been
115 shown to be geochemically very similar to OM at the head of the estuary (~ 350 km
116 downstream), consistent with no major tributaries joining the Congo River between
117 Malebo Pool and the Atlantic Ocean (Spencer et al., 2012). Annual water level
118 change in Malebo Pool is ~3 m and average river flow is ~30 000 m³ s⁻¹ during dry
119 periods and 60 000 m³ s⁻¹ during the wet season (Thieme et al., 2005).

120 During the Ocean Drilling Program (ODP) leg 175, 13 sites were drilled off the West
121 African coast (Aug-1997; Shipboard Scientific Party, 1998). ODP site 1075 is a deep
122 water drill site on a depth transect in the lower Congo basin located at 2995 m water
123 depth. ODP 1075 is dominated by (1) freshwater input from the Congo River, (2)

124 seasonal coastal upwelling activity and associated filaments and eddies moving
125 offshore, and (3) incursions of open-ocean waters from the South Equatorial
126 Countercurrent (Berger et al., 2002). Sediments from ODP 1075 and neighboring
127 cores (e.g. ODP 1077) have been closely correlated with climatic signaling (Jahn et
128 al., 2005) and large scale shifts in terrestrial vegetation relating to humidity – aridity
129 cycles (Dupont et al., 2000; Schefuß et al., 2003; 2004). ODP 1075 is approximately
130 200 m.b.s.f. with an average sedimentation rate of 100 m/Ma. OM in ODP 1075 is of
131 mixed terrestrial and marine origin, with soil OM (SOM) being an important but
132 variable contributor (Holtvoeth et al., 2001, 2003).

133 Sediment cores from ODP 1075 were stored at the International Ocean Discovery
134 Program (IODP) Bremen Core Repository (MARUM, Bremen University) at 4°C.
135 Samples between 1.65 and 115.65 m.b.s.f were previously collected by Holtvoeth et
136 al. (2001) and made available to this study. The lower section between 115.7-201.25
137 m.b.s.f of ODP 1075 (core A) were re-sampled at 1 m intervals, resolving on average
138 13 to 18 ka. The samples were stored in polypropylene bags and shipped to
139 Newcastle University (UK) where they were frozen immediately upon arrival.

140 **2.2. STRATIGRAPHY AND AGE MODEL**

141 Stratigraphy and the age model of ODP 1075 was previously determined by Dupont
142 et al. (2001). Due to low amounts of calcareous foraminifera in ODP 1075 for oxygen
143 isotope stratigraphy, the age model was established by correlating magnetic
144 susceptibility of 1075 with the neighboring site 1077. Both ODP sites 1075 and 1077
145 represent the same hydrographic conditions and show similar variations in magnetic
146 susceptibility (see Fig. 1 in Dupont et al., 2001). The age model for site 1077 is
147 based on a correlation of the $\delta^{18}\text{O}$ curve for *Globigerinoides ruber* (pink) with the
148 benthic isotope record of ODP site 677 in the deep Pacific (Shackleton et al., 1990).

149 Sedimentation rates were calculated by linear interpolation between age control
150 points (Jahn, 2002). The error associated with the age model of ODP 1075 has been
151 roughly estimated by Berger et al. (2002) to be approximately 0.01 Ma. The age
152 assignment of MIS are according to Lisiecki and Raymo (2005).

153 **2.3. TOTAL ORGANIC CARBON (TOC)**

154 Total OC (%) content of ODP 1075 samples between 115.7-201.25 m.b.s.f were
155 measured at Newcastle University using a LECO CS244 Carbon/Sulfur Analyser as
156 detailed in Spencer-Jones et al. (2015). TOC of samples between 1.65-115.65
157 m.b.s.f were obtained from Holtvoeth et al. (2003).

158 **2.4. LIPID EXTRACTION**

159 Total lipids were extracted using an adaptation of the method published in Talbot et
160 al. (2007) and further modified by Osborne (2016), which is based on the Kates
161 modification (Kates, 1972) of the Bligh and Dyer extraction (Bligh and Dyer, 1959).
162 Total lipids were extracted from 1-3 g of freeze-dried and homogenised sediment.
163 Sediment was extracted in a Teflon centrifuge tube (50 ml) with a monophasic
164 mixture of bi-distilled water (4 ml), methanol (10 ml) and chloroform (5 ml). The
165 sample was agitated vigorously via sonication for 15 min at 40°C followed by
166 centrifugation for 15 min at 12000 rpm. The supernatant was collected and added to
167 a second 50 ml centrifuge tube. This extraction was repeated three times with the
168 supernatant collected at the end of each extraction cycle.

169 The monophasic extracts were phase separated via addition of chloroform (5 ml) and
170 bi-distilled water (5 ml) to each of the supernatants. The sample was gently inverted
171 and centrifuged for 5 minutes (12000 rpm) to break the emulsion. The organic layer
172 from each tube was transferred to a round bottom flask (100 ml) and concentrated

173 using a rotary evaporator. The total lipid extract (TLE) was transferred to a glass vial
174 using chloroform/methanol at a ratio of 2:1 (v/v). A 5 α -pregnane-3 β ,20 β -diol internal
175 standard was added to the TLE. One third of the TLE was acetylated using acetic
176 anhydride (250 μ l) and pyridine (250 μ l). The TLE was heated at 50°C for one hour
177 and then left at room temperature overnight. Samples were dried under a stream of
178 N₂ with heating from below (40°C). BHP extracts were then stored at 4°C prior to
179 further processing.

180 **2.5. BACTERIOPANEPOLYOL ANALYSIS**

181 BHP analysis was performed by HPLC-APCI-MSⁿ using a ThermoFinnigan surveyor
182 HPLC system fitted with a Phenomenex Gemini C₁₈ column (150 mm; 3.0 mm i.d.; 5
183 μ m particle size) and a security guard column cartridge of the same material coupled
184 to a Finnigan LCQ ion-trap mass spectrometer equipped with an APCI source
185 operated in positive ion mode, as described in Talbot et al. (2003). The error in
186 absolute quantification was \pm 20%, based on selected replicate analyses and BHP
187 standards of known concentration (Cooke, 2010; van Winden et al., 2012b). The
188 abbreviated names of the compounds identified, characteristic base peak ions (*m/z*)
189 and structure numbers are given (Table 1). All concentrations are given to 2
190 significant figures with raw data presented in Appendix A. Statistical analysis was
191 performed using Minitab 17.1.0. Spearman's Rho (R_s) correlation index was
192 performed on BHP abundances. "CH₄ oxidation markers" is the sum of aminotetrol,
193 aminopentol, aminopentol isomer, and unsaturated aminopentol (**II**, **III**, **III'**, **IV/IV**). In
194 this study, we report 182 new BHP data points from the Congo deep-sea fan (ODP
195 site 1075) which are complemented by 122 data points published by Talbot et al.
196 (2014).

197 3. RESULTS

198 Consistent with Talbot et al. (2014), aminotriol (**I**), aminotetrol (**II**), aminopentol (**III**),
199 aminopentol isomer (**III'**), and unsaturated aminopentol (**IV** or **V**) are identified within
200 ODP 1075 sediments (Fig. 2a, b, c, and e). Aminotriol is the most abundant 35-
201 amino BHP with concentrations between 4.6 and 360 $\mu\text{g gTOC}^{-1}$. This is followed by
202 aminopentol as the second most abundant 35-amino BHP with concentrations
203 ranging between 0 and 280 $\mu\text{g gTOC}^{-1}$. Aminotetrol is identified at lower
204 concentrations, compared with aminotriol and aminopentol and is intermittently
205 present throughout ODP 1075. Despite differences in concentration, aminotriol,
206 aminotetrol, and aminopentol show similarities in distributions and persist to the
207 bottom of the core at 201.25 m.b.s.f (~ 2.5 Ma). In contrast, unsaturated aminopentol
208 (0 and 12 $\mu\text{g gTOC}^{-1}$) and aminopentol isomer (0 and 39 $\mu\text{g gTOC}^{-1}$) are present at
209 much lower concentrations and do not show a similar distribution to aminotriol,
210 aminotetrol and aminopentol (Fig. 2b and c). Significant correlation is found between
211 aminopentol and aminotriol (R_s 0.891, $p < 0.05$; Fig. 2e), aminopentol and aminotetrol
212 (R_s 0.908, $p < 0.05$; Fig. 2e), and aminotriol and aminotetrol (R_s 0.904, $p < 0.05$, not
213 shown), supporting a common response of all compounds to changing
214 environmental and/or depositional conditions. No statistically relevant correlation is
215 observed between TOC and aminotriol (R_s 0.101, p 0.079), aminotetrol (R_s -0.042, p
216 0.463), or aminopentol (R_s 0.006, p 0.920) concentrations ($\mu\text{g g sediment}^{-1}$; figures
217 not shown). Total CH_4 oxidation marker concentrations (sum **II**, **III**, **III'**, **IV/V**) are
218 highly variable down core (Fig. 2d). Peak concentrations in CH_4 oxidation markers
219 occur at around 1686 ka (270 $\mu\text{g gTOC}^{-1}$), 1271 ka (330 $\mu\text{g gTOC}^{-1}$) and 491 ka (270
220 $\mu\text{g gTOC}^{-1}$). Starting at the Pliocene/Pleistocene transition (~ 2.5 Ma), a steady
221 increase in CH_4 oxidation marker concentration is observed. Between 1865 and

222 1713 ka (hereafter referred to as interval 'a'; Fig. 2d) a clear decrease in CH₄
223 oxidation marker concentration is observed. A similar reduction in CH₄ oxidation
224 markers ($\mu\text{g gTOC}^{-1}$) is also observed between 1099 ka and 826 ka (hereafter
225 referred to as interval 'b'; Fig. 2d).

226 35-Amino BHPs show a similar distribution within the high resolution sections to the
227 full ODP 1075 record (Fig. 3 and Fig. 4). Aminotriol is the most abundant BHP (4.6
228 and 270 $\mu\text{g gTOC}^{-1}$) followed by aminopentol (0 and 210 $\mu\text{g gTOC}^{-1}$). Unsaturated
229 aminopentol and aminopentol isomer have an intermittent presence between MIS 2-
230 6 and MIS 10-13. Peak concentrations in aminotriol, aminotetrol, and aminopentol
231 are observed during MIS 5, 11, and 13, reaching comparable maximum levels for all
232 three warm intervals (Fig. 3 and Fig. 4). Similar to the overall BHP distribution in
233 ODP 1075 (Fig. 2), CH₄ oxidation marker concentrations are highly variable during
234 the investigated high resolution MIS intervals (Fig. 3 and Fig. 4). High concentrations
235 of total CH₄ oxidation markers are observed during MIS 13 (range 0 and 270 μg
236 gTOC^{-1} , mean 130 $\mu\text{g gTOC}^{-1}$), followed by a reduction during MIS 12 (range 0 and
237 210 $\mu\text{g gTOC}^{-1}$, mean 51 $\mu\text{g gTOC}^{-1}$), and a marked increase in CH₄ oxidation
238 markers during MIS 11 (range 0 and 260 $\mu\text{g gTOC}^{-1}$, mean 96 $\mu\text{g gTOC}^{-1}$). Peak
239 concentration in CH₄ oxidation marker is similar during MIS 11 and 13 (Fig. 3). Low
240 concentrations of CH₄ oxidation markers are observed during MIS 6 (range 0 and 39
241 $\mu\text{g gTOC}^{-1}$, mean 14 $\mu\text{g gTOC}^{-1}$) followed by an increase in concentration during MIS
242 5 (range 5.7 and 190 $\mu\text{g gTOC}^{-1}$, mean 66 $\mu\text{g gTOC}^{-1}$). Following MIS 5, CH₄
243 oxidation marker concentration remains low during MIS 2-4 (range 0 and 96 μg
244 gTOC^{-1} , mean 14 $\mu\text{g gTOC}^{-1}$). Overall higher mean CH₄ oxidation markers are
245 observed during MIS 11 and 13 compared with MIS 5 (Fig. 5).

246 4. DISCUSSION

247 4.1. DIAGENETIC AND ENVIRONMENTAL CONTROLS ON 35-AMINO BHPS 248 IN ODP 1075

249 Aminotriol (I), aminotetrol (II) and aminopentol (III) down core profiles do not show
250 clear diagenetic trends, with all of these compounds present within ODP 1075
251 sediments dated to ~ 2.5 Ma (Fig. 2). The absence of any correlation between TOC
252 and 35-amino BHP suggests that variations in BHPs are not driven by variations in
253 TOC. One previous study exists discussing the preservation of 35-amino BHPs in
254 ancient sediments, where Wagner et al. (2014) identified CH₄ oxidation markers in
255 Amazon fan and shelf sediments to a maximum core depth of 708 cm, dated to
256 approximately 30 ka. The results shown here from the Congo deep-sea fan
257 represent the oldest and longest continuous record of CH₄ oxidation markers in
258 sediments to date. As no clear diagenetic trend in CH₄ oxidation markers is evident
259 we anticipate that these biomarkers can be examined within much deeper
260 sediments, without any reasonable justification for a specific sub-surface limit.
261 Furthermore, we also report the occurrence of unsaturated aminopentol and
262 aminopentol isomer within sediments dating to 2.2 Ma and 2.4 Ma, respectively (Fig.
263 2). The observation of unsaturated aminopentol and aminopentol isomer in ODP
264 1075, again, is the oldest reported occurrence of these two compounds, building
265 confidence that the high resolution 35-amino BHP records presented here represent
266 primary signals, with minimal or no diagenetic alteration.

267 Previous analysis of 35-amino BHPs within Congo fan sediments suggest that these
268 compounds are of allochthonous origins, likely derived from Congo hinterland
269 wetlands and similar environments (Talbot et al., 2014). In agreement with previous
270 studies, BHP concentrations and proportions of aminotriol:aminopentol:aminotetrol in

271 our extended ODP 1075 record show strong correlation to each other (Fig. 2e; Cvejic
272 et al., 2000; Talbot et al., 2001; van Winden et al., 2012b; Osborne, 2016) supporting
273 a common methanotroph source.

274 **4.2. A 2.5 MA RECORD OF CH₄ CYCLING**

275 As discussed in Talbot et al. (2014), analysis of Congo fan sediments suggests long
276 term fluctuations in CH₄ oxidation markers during the Pleistocene with enhanced
277 production and preservation of CH₄ oxidation markers during warm-humid
278 interglacial MIS. The data presented here, support and further expand this concept.
279 Intervals 'a' and 'b' (Fig. 2d), suggest a shift in the terrestrial BHP producing
280 community and thus widespread change in African ecology and hydrology that
281 coincides with increased African climate variability and aridity between 1.7 Ma and 1
282 Ma (deMenocal, 2004; Trauth et al., 2007). We propose that increased continental
283 African aridity would have reduced wetland extent and, subsequently, reduced the
284 production and supply of CH₄ oxidation markers to the Congo fan. These arid
285 intervals of low CH₄ oxidation marker concentrations are consistent with the onset
286 and amplification of high latitude glacial conditions (deMenocal et al., 1993, 1995;
287 Tiedemann et al., 1994; Clemens et al., 1996). Furthermore, CH₄ oxidation markers
288 have been shown to follow a systematic pattern of elevated concentrations during
289 warm MIS 5, 11, 13, 17, 21, and 33 (Talbot et al., 2014). Our study further supports
290 this trend and shows that this relationship persists beyond 1.2 Ma to 2.5 Ma with
291 high concentrations of CH₄ oxidation markers identified during MIS 39, 47, 49, 59,
292 75, and 83 (Fig. 2). This new data further suggests enhanced methane cycling
293 during warm-humid time periods of the Pleistocene.

294 **4.3. SHORT TERM TRENDS IN CH₄ CYCLING**

295 Throughout the Pleistocene, subtropical African climate periodically oscillated
296 between wet and dry climate conditions, which drove largescale ecological change
297 (Scheffuß et al., 2003, 2005; deMenocal, 2004). The high resolution timeseries of
298 MIS 5, 11, and 13 show high concentrations of CH₄ oxidation markers, consistent
299 with high global GHG concentrations (Fig. 3 and 4) and suggest enhanced C cycling
300 during these intervals. Furthermore, high concentrations of these biomarkers coincide
301 with the expansion of tropical rainforests and water-dependent ecosystems (Miller
302 and Gosling, 2014) supporting the concept that CH₄ oxidation markers may actually
303 document widespread ecological change in the Congo.

304 Global methane concentrations were high during MIS 5 and MIS 11 (Fig. 3 and 4)
305 and slightly lower during MIS 13, largely owing to a cooler climate (Spahni et al.,
306 2005). However, the range of CH₄ oxidation marker concentrations in the Congo
307 core are comparable for all three time slices (Fig. 3 and 4), suggesting either
308 similarities in methanotrophy/ecosystem and/or a decoupling between BHP
309 synthesis and aerobic methanotrophy.

310 **4.3.1. WEST AFRICAN ECOSYSTEM DURING THE PLEISTOCENE**

311 Similarities in methanotrophy/ecosystem during MIS 5, 11, and 13 are supported by
312 integrated palynological evidence from various sediment cores from the wider West
313 African coastal area suggesting strong similarities in vegetation, habitat types, and
314 interpreted temperatures and precipitation (Miller and Gosling, 2014). Furthermore,
315 fluctuations in global atmospheric CH₄ concentrations may have been due to
316 changes in Northern hemisphere methane sources (Froese et al., 2008; Vaks et al.,
317 2010; Vázquez Riveiros et al., 2013; Reyes et al., 2014), therefore not directly
318 affecting tropical wetland sources and thus BHP signatures in deep-sea fan settings.

319 Low concentrations of CH₄ oxidation marker are observed during MIS 2, 3, 4, 6, 10,
320 12, which also coincides with globally low concentrations of atmospheric GHG and
321 would support the development of dry-arid conditions (Spahni et al., 2005), with
322 restricted extent of water dependent ecosystems (Dalibard et al., 2014). While
323 wetland ecosystems are not well represented within the palynological archive, pollen
324 records can indicate ecosystem community structure and potential environmental
325 conditions (for example, Miller and Gosling, 2014). Limited evidence from pollen
326 records from the tropical Atlantic off West Africa indeed indicates that vegetation
327 assemblages of the Congo basin and surrounding mountains were susceptible to
328 changes in precipitation during the Pleistocene, with extensive rainforest and
329 mangrove ecosystems common during humid stages (Dalibard et al., 2014). The
330 development of more open, savannah-type ecosystems is characteristic of glacial
331 periods (Dupont et al., 2000; Versteegh et al., 2004; Dupont, 2009), supporting our
332 conclusion of a reduction in wetland habitats during these overall dryer periods.

333 Progressively lower mean CH₄ oxidation marker concentrations are observed during
334 MIS 5 compared with the older warm isotope stages (i.e. MIS 11 and 13; Fig. 5). This
335 is despite MIS 5 being considered a very warm interglacial with high global
336 atmospheric methane concentrations (Spahni et al., 2005; Loulergue et al., 2008).

337 This disparity may suggest more extended wetlands during MIS 11, 13, and
338 potentially earlier interglacial climate stages of the Pleistocene, compared to MIS 5.

339 Terrestrial and marine paleoclimate records from Africa suggest a trend towards
340 greater aridity during the Pleistocene (Schefuß et al., 2003; deMenocal, 2004;
341 Ségalen et al., 2007; Trauth et al., 2009) consistent with shifts in vegetation from C3
342 (trees and shrubs) to C4 (tropical grasses). However, despite the global trend
343 towards greater aridity, regional/local trends may have diverged showing more

344 pronounced variability and higher frequency alternating between dry and humid
345 periods (e.g. Johnson et al., 2016).

346 **4.3.2. DECOUPLING OF BHP SYNTHESIS AND GLOBAL GREENHOUSE** 347 **GAS CONCENTRATIONS**

348 In addition to climatological and hydrological driven changes in Congo carbon
349 cycling, CH₄ oxidation marker concentrations could also show a potential decoupling
350 between aerobic methanotrophy, BHP synthesis, and atmospheric GHG
351 concentrations. Support for this concept comes from incubations of enrichment
352 cultures that show temperature variations having a strong control on AMO intensity,
353 with peak methane oxidation occurring between 20 and 40°C (van Winden, 2011;
354 Sherry et al., 2016) and resulting in a shift in methanotroph community structure (e.g.
355 Sherry et al., 2016). Furthermore, aerobic methanotroph activity appears closely
356 controlled by the heterogeneity in the soil environment, the solubility and
357 bioavailability of methane - a direct variable linked to methane production and
358 methane flux - and other environmental parameters (e.g. pH, salinity; Sherry et al.,
359 2016). Climate and hydrology cycles were highly variable during the Pleistocene,
360 with MIS 13 relatively cool and arid and MIS 5 and 11 relatively warm and humid
361 (Spahni et al., 2005). These differences could have resulted in differences in carbon
362 cycling and resulted in the BHP concentrations observed in Fig. 2, 3, and 4. Under
363 the warm and humid environmental conditions of MIS 5 and 11, the ecosystem
364 would have supported extended wetlands with intense methanogenesis. Aerobic
365 methanotrophy could have decreased through a potential reduction in the oxic-
366 anoxic boundary or through the methanotroph community being bypassed due to the
367 sudden release of methane bubbles (ebullition, e.g. Bastviken et al., 2004) and/or
368 plant mediated transport of methane gas to the atmosphere (Whalen, 2005). The

369 degree to which these parameters control BHP synthesis as well as preservation
370 within marine sediments is still largely unknown (Jahnke et al., 1999; Poralla et al.,
371 2000; Doughty et al., 2009; Welander et al., 2009; van Winden, 2011).

372 **4.4. TRANSPORT, DEPOSITION, AND AGE OF BHP RECORDS IN THE** 373 **CONGO DEEP-SEA FAN**

374 We recognise two principal challenges to constrain the sensitivity of CH₄ oxidation
375 markers in the deep-sea fan within the context of West African climate dynamics.

376 These are (1) the mechanisms and locations of aminopentol signal formation and its
377 transport and burial in the deep marine sediments and (2) a robust high resolution
378 stratigraphic framework to place possible mechanisms into the climatic and
379 sedimentological context of the African-Congo catchment/deep-sea fan system.

380 Here, we further discuss these control mechanisms within a conceptual framework
381 for further research.

382 **4.4.1. TRANSPORT AND DEPOSITION OF BHP SIGNAL IN THE CONGO** 383 **CATCHMENT**

384 Previous endmember analysis suggests that the source of Congo methane oxidation
385 signature may indeed come from the deep interior of the Congo catchment
386 (Spencer-Jones et al., 2015), and is potentially controlled by central African climate
387 evolution (Schefuß et al., 2016). However, the extent to which the biomarker signal is
388 reworked during transport from source environments to the Congo fan is yet to be
389 elucidated. During riverine transport, a large proportion of sediment is trapped on the
390 Cuvette Centrale with a lesser proportion of sediment subsequently trapped at
391 Malebo pool (Laraque et al., 2009; Spencer et al., 2012). Furthermore, the fine
392 particulate organic matter (FPOM, 0.7-63µm) fraction potentially undergoes some

393 form of extended degradation in the Cuvette Centrale (Laraque et al., 2009; Spencer
394 et al., 2012). However, Spencer et al. (2012) found little evidence to suggest
395 degradation or variation in the FPOM fraction at the mainstem sites before and after
396 Malebo pool on the Congo River. Therefore, it remains unclear to what extent the
397 BHP component of FPOM may be reworked in the Cuvette Centrale prior to delivery
398 on the Congo fan. The biomarker signal may also be influenced by changes in the
399 topography and run-off patterns as the landscape of the catchment evolved
400 throughout the late Quaternary, possibly with more direct export during earlier
401 interglacial phases in comparison to their more recent analogues.

402 **4.4.2. LAGS IN BIOMARKER RESPONSE**

403 For some but not all glacial-interglacial transitions a delay in biomarker response is
404 noted (e.g. transition from MIS 12-11 in Fig. 4). During MIS 11 a decrease in CH₄
405 oxidation marker concentration is observed at 388 ka which is 15 ka prior to the
406 beginning of MIS 10. This delay appears to be long taking other studies addressing
407 lead-lag relationships in the Congo system into consideration (e.g. Schneider et al.,
408 1995; Zabel et al., 2001; Holtvoeth et al., 2003) therefore we assume that this is a
409 result of uncertainties in the age model during that specific time period (see section
410 2.2). Schneider et al. (1995) and Dupont et al. (1999) demonstrated that fluctuations
411 in SST, salinity, runoff, upwelling, organic carbon burial and vegetation in the Congo
412 catchment were in phase and highly sensitive to climate forcing at orbital 23- and
413 100-kyr periodicities, but did not follow the pacing of global ice-volume and glacial
414 stages, emphasizing the relevance of monsoonal impact on tropical climate systems.
415 The response of the terrestrial biome to climate and hydrological change may
416 possibly have resulted in leads and lags in biomarker response on shorter
417 timescales. Holtvoeth et al. (2003) reports a 2-4 ka time shift of bulk organic

418 geochemical signatures that correspond to the delayed development of vegetation
419 and soil with respect to atmospheric circulation and insolation, however, the absolute
420 duration of the lag remains unclear within the context of the error associated with the
421 age model of ODP 1075 (see section 2.2). This lag is supported by Zabel et al.
422 (2001), who observe lags between the fluctuation in the suspension load of the Niger
423 River and insolation during the Pleistocene where oscillation of solar radiation led
424 variations of the terrigenous composition by ~4100-5100 yr. In addition to the age
425 model limitations between the comparison of GHG and biomarker records, lag time
426 between vegetation build up and rapid warming, and temporary storage (pre-aging)
427 of the terrestrial carbon within the catchment (Schefuß et al., 2016) may also need to
428 be taken into account when interpreting the observed time differences in the GHG
429 and aminopentol records.

430 **5. CONCLUSIONS**

431 35-amino BHPs including aminotriol, aminotetrol and aminopentol are found in high
432 concentrations throughout ODP 1075 to a maximal depth of 201.25 m.b.s.f.,
433 equivalent to ~2.5 Ma. This represents the oldest record of 35-amino BHPs and
434 suggests that these biomarkers may well be preserved in much deeper and older
435 sedimentary archives. Low concentrations of CH₄ oxidation markers, identified
436 between 1865 and 1713 ka ('a') and 1099 and 826 ka ('b'), suggest a reduction in
437 wetland extent in response to more arid tropical African environmental conditions,
438 consistent with a reported increase in climate variability and aridity near 1.7 Ma and
439 1 Ma. Correlation of high resolution CH₄ oxidation marker signatures with global
440 atmospheric methane concentrations during MIS 5, 11, and 13 further suggests
441 periods of enhanced tropical methane cycling. Furthermore, we observe a
442 decoupling between CH₄ oxidation marker concentrations and atmospheric GHG

443 concentrations potentially due to a range of physical (West African climate and
444 hydrological cycles) and/or biological parameters impacting on the tropical C cycle.
445 Moreover, subsequent analysis is required to extrapolate the relative importance of
446 tropical methane sources as a driver of global methane concentrations observed in
447 ice core records.

448 **ACKNOWLEDGMENTS**

449 We are grateful for funding from the European Research Council for a starting grant
450 (258734) awarded to H.M.T. for project AMOPROX. We thank the Natural
451 Environment Research Council (NERC) for funding (Grant number NE/E017088/1)
452 and the International Ocean Discovery Program (IODP) for supplying sediments. We
453 also thank F. Sidgwick and P. Green for technical support. We thank the Science
454 Research Investment Fund (SRIF) from the UK HEFCE for funding the purchase of
455 the ThermoFinnigan LCQ ion trap mass spectrometer. We thank Lydie Dupont for
456 constructive feedback. We also thank the associate editor (E. Hornibrook) and three
457 anonymous reviewers for constructive feedback.

458

459 **References**

460 Anka Z. and Séranne M. (2004) Reconnaissance study of the ancient Zaire (Congo)
461 deep-sea fan (ZaiAngo Project). *Mar. Geol.* **209**, 223-244.

462 Bartlett K. B. and Harriss R. C. (1993) Review and assessment of methane
463 emissions from wetlands. *Chemosphere* **26**, 261-320.

464 Bastviken D., Cole J., Pace M. and Tranvik L. (2004) Methane emissions from lakes:
465 Dependence of lake characteristics, two regional assessments, and a global
466 estimate. *Glob. Biogeochem. Cycle* **18** DOI; 10.1029/2004gb002238

467 Berger W. H., Lange C. B. and Wefer G. (2002) Upwelling history of the Benguela-
468 Namibia system: A synthesis of Leg 175 Results. Available from the World Wide
469 Web: <http://www-odp.tamu.edu/publications/175_SR/synth/synth.htm> [Cited 2015-
470 03-05].

- 471 Berndmeyer C., Thiel V., Schmale O. and Blumenberg M. (2013) Biomarkers for
472 aerobic methanotrophy in the water column of the stratified Gotland Deep (Baltic
473 Sea). *Org. Geochem.* **55**, 103-111.
- 474 Bligh E. G. and Dyer W. J. (1959) A rapid method of total lipid extraction and
475 purification. *Canadian J. Biochem. Physiol.* **37**, 911-917.
- 476 Blumenberg M., Seifert R. and Michaelis W. (2007) Aerobic methanotrophy in the
477 oxic-anoxic transition zone of the Black Sea water column. *Org. Geochem.* **38**, 84-
478 91.
- 479 Blunier T., Chappellaz J., Schwander J., Stauffer B. and Raynaud D. (1995)
480 Variations in atmospheric methane concentration during the Holocene epoch. *Nature*
481 **374**, 46-49.
- 482 Bwangoy J. R. B., Hansen M. C., Roy D. P., De Grandi G. and Justice C. O. (2010)
483 Wetland mapping in the Congo Basin using optical and radar remotely sensed data
484 and derived topographical indices. *Remote Sens. Environ.* **114**, 73-86.
- 485 Clemens S. C., Murray D. W. and Prell W. L. (1996) Nonstationary phase of the plio-
486 pleistocene Asian monsoon. *Science* **274**, 943-948.
- 487 Cooke M. P. (2010) The Role of Bacteriohopanepolyols as Biomarkers for Soil
488 Bacterial Communities and Soil Derived Organic Matter, Civil Engineering and
489 Geoscience. Newcastle University (UK), PhD Thesis.
- 490 Coolen M. J. L., Talbot H. M., Abbas B. A., Ward C., Schouten S., Volkman J. K. and
491 Sinninghe Damsté J. S. (2008) Sources for sedimentary bacteriohopanepolyols as
492 revealed by 16S rDNA stratigraphy. *Environ. Microbiol.* **10**, 1783-1803.
- 493 Cvejjic J. H., Bodrossy L., Kovács K. L. and Rohmer M. (2000) Bacterial triterpenoids
494 of the hopane series from the methanotrophic bacteria *Methylocaldum* spp.:
495 Phylogenetic implications and first evidence for an unsaturated
496 aminobacteriohopanepolyol. *FEMS Microbiol. Lett.* **182**, 361-365.
- 497 Dalibard M., Popescu S. M., Maley J., Baudin F., Melinte-Dobrinescu M. C., Pittet B.,
498 Marsset T., Dennielou B., Droz L. and Suc J. P. (2014) High-resolution vegetation
499 history of West Africa during the last 145 ka. *Geobios* **47**, 183-198.
- 500 deMenocal P. B. (1995) Plio-Pleistocene African climate. *Science* **270**, 53-59.
- 501 deMenocal P. B. (2004) African climate change and faunal evolution during the
502 Pliocene-Pleistocene. *Earth Planet. Sci. Lett.* **220**, 3-24.
- 503 deMenocal P. B., Ruddiman W. F. and Pokras E. M. (1993) Influence of high- and
504 low-latitude processes on African terrestrial climate: Pleistocene eolian records from
505 equatorial Atlantic Ocean Drilling Program Site 663. *Paleoceanography* **8**, 209-242.
- 506 Doughty D. M., Hunter R. C., Summons R. E. and Newman D. K. (2009) 2-
507 Methylhopanoids are maximally produced in akinetes of *Nostoc punctiforme*:
508 Geobiological implications. *Geobiology* **7**, 524-532.

- 509 Dupont L. M. (2009) The Congo deep-sea fan as an archive of Quaternary change in
 510 Africa and the eastern tropical south Atlantic (a review), in: Kneller, B., Martinsen,
 511 O.J., McCaffrey, B. (Eds.), *External Controls on Deep-Water Depositional Systems*.
 512 S E P M - Soc Sedimentary Geology, Tulsa, pp. 79-87.
- 513 Dupont L. M., Bonner B., Schneider R. and Wefer G. (2001) Mid-Pleistocene
 514 environmental change in tropical Africa began as early as 1.05 Ma. *Geology* **29**, 195-
 515 198.
- 516 Dupont L. M., Jahns S., Marret F. and Ning S. (2000) Vegetation change in
 517 equatorial West Africa: Time-slices for the last 150 ka. *Palaeogeogr. Palaeoclimatol.*
 518 *Palaeoecol.* **155**, 95-122.
- 519 Dupont, L.M., Schmäuser, A., Jahns, S. and Schneider, R. (1999) Marine - terrestrial
 520 interaction of climate changes in West Equatorial Africa of the last 190,000 years.
 521 *Palaeoecology of Africa* 26, 61-84.
- 522 Eickhoff M., Birgel D., Talbot H. M., Peckmann J. and Kappler A. (2013)
 523 Bacteriohopanoid inventory of *Geobacter sulfurreducens* and *Geobacter*
 524 *metallireducens*. *Org. Geochem.* **58**, 107-114.
- 525 Froese D. G., Westgate J. A., Reyes A. V., Enkin R. J. and Preece S. J. (2008)
 526 Ancient permafrost and a future, warmer arctic. *Science* **321**, 1648.
- 527 Holtvoeth J., Wagner T., Horsfield B., Schubert C. J. and Wand U. (2001) Late-
 528 quaternary supply of terrigenous organic matter to the Congo deep-sea fan (ODP
 529 site 1075): Implications for equatorial African paleoclimate. *Geo-Mar. Lett.* **21**, 23-33.
- 530 Holtvoeth J., Wagner T. and Schubert C. J. (2003) Organic matter in river-influenced
 531 continental margin sediments: The land-ocean and climate linkage at the Late
 532 Quaternary Congo fan (ODP Site 1075). *Geochem. Geophys. Geosyst.* **4**, DOI:
 533 10.1029/2003gc000590.
- 534 Howard W. R. (1997) A warm future in the past. *Nature* **388**, 418-419.
- 535 IPCC (2013) Climate change 2013: The Physical Science Basis. Contribution of
 536 working group I to the fifth assessment report of the intergovernmental panel on
 537 climate change, Cambridge university press, Cambridge, United Kingdom and New
 538 York, NY, USA.
- 539 Jahn B. (2002) Mid to Late Pleistocene Variations of Marine Productivity in and
 540 Terrigenous Input to the Southeast Atlantic, Berichte, Fachbereich
 541 Geowissenschaften. Universität Bremen. PhD Thesis.
- 542 Jahn B., Schneider R. R., Muller P. J., Donner B. and Rohl U. (2005) Response of
 543 tropical African and East Atlantic climates to orbital forcing over the last 1.7 Ma, in:
 544 Head, M.J., Gibbard, P.L. (Eds.), *Early-Middle Pleistocene Transitions: The Land-
 545 Ocean Evidence*. Geological Soc Publishing House, Bath, pp. 65-84.
- 546 Jahnke L. L., Summons R. E., Hope J. M. and Des Marais D. J. (1999) Carbon isotopic
 547 fractionation in lipids from methanotrophic bacteria II: The effects of physiology and
 548 environmental parameters on the biosynthesis and isotopic signatures of biomarkers.

- 549 *Geochim. Cosmochim. Acta* **63**, 79-93.
- 550 Johnson, T.C., Werne, J.P., Brown, E.T., Abbott, A., Berke, M., Steinman, B.A., Halbur, J.,
551 Contreras, S., Grosshuesch, S., Deino, A., Lyons, R.P., C.A., S., S., S. and Sinninghe
552 Damsté, J.S. (2016) A progressively wetter climate in southern East Africa over the past 1.3
553 million years. *Nature*. **537**, 220-224.
- 554 Kates M. (1972) Techniques of lipidology: isolation, analysis and identification of
555 lipids. North-Holland Publishing Company, Amsterdam.
- 556 Kukla G., McManus J. F., Rousseau D. D. and Chuine I. (1997) How long and how
557 stable was the last interglacial? *Quat. Sci. Rev.* **16**, 605-612.
- 558 Laraque A., Bricquet J. P., Pandi A. and Olivry J. C. (2009) A review of material
559 transport by the Congo River and its tributaries. *Hydrol. Process.* **23**, 3216-3224.
- 560 Lisiecki L. E. and Raymo M. E. (2005) A Pliocene-Pleistocene stack of 57 globally
561 distributed benthic delta O-18 records. *Paleoceanography* **20**, DOI:
562 10.1029/2004pa001071.
- 563 Loulergue L., Schilt A., Spahni R., Masson-Delmotte V., Blunier T., Lemieux B.,
564 Barnola J.-M., Raynaud D., Stocker T. F. and Chappellaz J. (2008) Orbital and
565 millennial-scale features of atmospheric CH₄ over the past 800,000 years. *Nature*
566 **453**, 383-386.
- 567 Loutre M. F. and Berger A. (2003) Marine Isotope Stage 11 as an analogue for the
568 present interglacial. *Global Planet. Change* **36**, 209-217.
- 569 Lüthi D., Le Floch M., Bereiter B., Blunier T., Barnola J. M., Siegenthaler U.,
570 Raynaud D., Jouzel J., Fischer H., Kawamura K. and Stocker T. F. (2008) High-
571 resolution carbon dioxide concentration record 650,000-800,000 years before
572 present. *Nature* **453**, 379-382.
- 573 Miller C. S. and Gosling W. D. (2014) Quaternary forest associations in lowland
574 tropical West Africa. *Quat. Sci. Rev.* **84**, 7-25.
- 575 Osborne K. A. (2016) Environmental Controls on Bacteriohopanepolyol Signatures in
576 Estuarine Sediment, Civil Engineering and Geoscience. Newcastle University (UK),
577 PhD Thesis.
- 578 Poralla K., Muth G. and Härtner T. (2000) Hopanoids are formed during transition
579 from substrate to aerial hyphae in *Streptomyces coelicolor* A3(2). *FEMS Microbiol.*
580 *Lett.* **189**, 93-95.
- 581 Petit J. R., Jouzel J., Raynaud D., Barkov N. I., Barnola J. M., Basile I., Bender M.,
582 Chappellaz J., Davis M., Delaygue G., Delmotte M., Kotlyakov V. M., Legrand M.,
583 Lipenkov V. Y., Lorius C., Pepin L., Ritz C., Saltzman E. and Stievenard M. (1999)
584 Climate and atmospheric history of the past 420,000 years from the Vostok ice core,
585 Antarctica. *Nature* **399**, 429-436.
- 586 Reyes A. V., Carlson A. E., Beard B. L., Hatfield R. G., Stoner J. S., Winsor K.,
587 Welke B. and Ullman D. J. (2014) South Greenland ice-sheet collapse during Marine
588 Isotope Stage 11. *Nature* **510**, 525-528.

- 589 Rohmer M., Bouviernave P. and Ourisson G. (1984) Distribution of hopanoid
590 triterpenes in prokaryotes. *J. Gen. Microbiol.* **130**, 1137-1150.
- 591 Rommerskirchen F., Eglinton G., Dupont L. and Rullkotter J. (2006)
592 Glacial/interglacial changes in southern Africa: Compound-specific delta C-13 land
593 plant biomarker and pollen records from southeast Atlantic continental margin
594 sediments. *Geochem. Geophys. Geosyst.* **7**, 21.
- 595 Runge J. (2007) The Cong River, Central Africa, in: Gupta, A. (Ed.), *Large Rivers:*
596 *Geomorphology and Management*. Wiley.
- 597 Sáenz J. P., Eglinton T. I. and Summons R. E. (2011) Abundance and structural
598 diversity of bacteriohopanepolyols in suspended particulate matter along a river to
599 ocean transect. *Org. Geochem.* **42**, 774-780.
- 600 Schefuß E., Eglinton T. I., Spencer-Jones C. L., Rullkötter J., De Pol Holz R., Talbot
601 H. M., Grootes P. M., Schneider R. R. (2016) Hydrologic control of carbon cycling
602 and aged carbon discharge in the Congo River basin. *Nature Geosci* **9**, 687-690.
- 603 Schefuß E., Schouten S., Jansen J. H. F. and Sinninghe Damsté J. S. (2003) African
604 vegetation controlled by tropical sea surface temperatures in the mid-Pleistocene
605 period. *Nature* **422**, 418-421.
- 606 Schefuß E., Schouten S. and Schneider R. R. (2005) Climatic controls on central
607 African hydrology during the past 20,000 years. *Nature* **437**, 1003-1006.
- 608 Schefuß E., Versteegh G. J. M., Jansen J. H. F. and Sinninghe Damsté J.S. (2004)
609 Lipid biomarkers as major source and preservation indicators in SE Atlantic surface
610 sediments. *Deep-Sea Res., Part I* **51**, 1199-1228.
- 611 Schneider R. R., Müller P. J. and Ruhland G. (1995) Late Quaternary Surface
612 Circulation in the East Equatorial South-Atlantic - Evidence from Alkenone Sea-
613 Surface Temperatures. *Paleoceanography* **10**, 197-219.
- 614 Ségalen L., Lee-Thorp J. A. and Cerling T. (2007) Timing of C4 grass expansion
615 across sub-Saharan Africa. *J. Hum. Evol.* **53**, 549-559.
- 616 Shackleton N. J., Berger A. and Peltier W. R. (1990) An Alternative Astronomical
617 Calibration of the Lower Pleistocene Timescale Based on Odp Site 677. *T Roy Soc*
618 *Edin-Earth* **81**, 251-261.
- 619 Sherry A., Osborne K. A., Sidgwick F. R., Gray N. D. and Talbot H. M. (2016) A
620 temperate river estuary is a sink for methanotrophs adapted to extremes of pH,
621 temperature and salinity. *Environ. Microbiol. Rep.* **8**, 122-131.
- 622 Shipboard Scientific Party (1998). Proceedings of the Ocean Drilling Program, Initial
623 Reports, 175. Ocean Drilling Program, College Station, Texas.
- 624 Singarayer J. S., Valdes P. J., Friedlingstein P., Nelson S. and Beerling D. J. (2011)
625 Late Holocene methane rise caused by orbitally controlled increase in tropical
626 sources. *Nature* **470**, 82-91.

- 627 Sjögersten S., Black C. R., Evers S., Hoyos-Santillan J., Wright E.L. and Turner B. L.
628 (2014) Tropical wetlands: A missing link in the global carbon cycle? *Global*
629 *Biogeochem. Cycles* **28**, 1371-1386.
- 630 Spahni R., Chappellaz J., Stocker T. F., Loulergue L., Hausammann G., Kawamura
631 K., Fluckiger J., Schwander J., Raynaud D., Masson-Delmotte V. and Jouzel J.
632 (2005) Atmospheric methane and nitrous oxide of the late Pleistocene from Antarctic
633 ice cores. *Science* **310**, 1317-1321.
- 634 Spencer R. G. M., Hernes P. J., Aufdenkampe A. K., Baker A., Gulliver P., Stubbins
635 A., Aiken G. R., Dyda R. Y., Butler K. D., Mwamba V. L., Mangangu A. M.,
636 Wabakanghanzi J. N. and Six J. (2012) An initial investigation into the organic matter
637 biogeochemistry of the Congo River. *Geochim. Cosmochim. Acta* **84**, 614-627.
- 638 Spencer-Jones C. L., Wagner T., Dinga B. J., Schefuß E., Mann P. J., Poulsen J. R.,
639 Spencer R. G. M., Wabakanghanzi J. N. and Talbot H. M. (2015)
640 Bacteriohopanepolyols in tropical soils and sediments from the Congo River
641 catchment area. *Org. Geochem.* **89-90**, 1-13.
- 642 Talbot H. M. and Farrimond P. (2007) Bacterial populations recorded in diverse
643 sedimentary biohopanoid distributions. *Org. Geochem.* **38**, 1212-1225.
- 644 Talbot H. M., Handley L., Spencer-Jones C. L., Biennu D. J., Schefuß E., Mann P.
645 J., Poulsen J. R., Spencer R. G. M., Wabakanghanzi J. N. and Wagner T. (2014)
646 Variability in aerobic methane oxidation over the past 1.2Myrs recorded in microbial
647 biomarker signatures from Congo fan sediments. *Geochim. Cosmochim. Acta* **133**,
648 387-401.
- 649 Talbot H. M., McClymont E., Inglis G. N., Evershed E. P., Pancost R. D. (2016)
650 Origin and preservation of bacteriohopanepolyol signatures in *Sphagnum* peat from
651 Bissendorfer moor (Germany). *Org. Geochem.* **97**, 95-110.
- 652 Talbot H. M., Squier A. H., Keely B. J. and Farrimond P. (2003) Atmospheric
653 pressure chemical ionisation reversed-phase liquid chromatography/ion trap mass
654 spectrometry of intact bacteriohopanepolyols. *Rapid Commun. Mass Spectrom.* **17**,
655 728-737.
- 656 Talbot H. M., Summons R. E., Jahnke L. L., Cockell C. S., Rohmer M. and
657 Farrimond P. (2008) Cyanobacterial bacteriohopanepolyol signatures from cultures
658 and natural environmental settings. *Org. Geochem.* **39**, 232-263.
- 659 Talbot H. M., Watson D. F., Murrell J. C., Carter J. F. and Farrimond P. (2001)
660 Analysis of intact bacteriohopanepolyols from methanotrophic bacteria by reversed-
661 phase high-performance liquid chromatography-atmospheric pressure chemical
662 ionisation mass spectrometry. *J. Chromatogr. A* **921**, 175-185.
- 663 Thieme M.L., Abell R., Burgess N., Lehner B., Dinerstein E., Olson D., Teugels G.,
664 Kamdem-Toham A., Stiassny M.L.J.S. and Skelton P. (2005) Freshwater Ecoregions
665 of Africa and Madagascar. Island Press, Washington DC.

- 666 Tiedemann R., Sarnthein M. and Shackleton N. J. (1994) Astronomic timescale for
667 the Pliocene Atlantic $\delta^{18}\text{O}$ and dust flux records of Ocean Drilling Program site 659.
668 *Paleoceanography* **9**, 619-638.
- 669 Trauth M. H., Larrasoana J. C. and Mudelsee M. (2009) Trends, rhythms and events
670 in Plio-Pleistocene African climate. *Quat. Sci. Rev.* **28**, 399-411.
- 671 Trauth M. H., Maslin M. A., Deino A. L., Strecker M. R., Bergner A. G. N. and
672 Dühnforth M. (2007) High- and low-latitude forcing of Plio-Pleistocene East African
673 climate and human evolution. *J. Hum. Evol.* **53**, 475-486.
- 674 Vaks A., Bar-Matthews M., Matthews A., Ayalon A. and Frumkin A. (2010) Middle-
675 Late Quaternary paleoclimate of northern margins of the Saharan-Arabian Desert:
676 reconstruction from speleothems of Negev Desert, Israel. *Quat. Sci. Rev.* **29**, 2647-
677 2662.
- 678 van Winden J. F. (2011) Methane Cycling in Peat Bogs: Environmental Relevance of
679 Methanotrophs Revealed by Microbial Lipid Chemistry. LPP Contribution Series (35).
680 Utrecht University.
- 681 van Winden J. F., Talbot H. M., De Vleeschouwer F., Reichart G. -J. and Sinninghe
682 Damsté J. S. (2012a) Variation in methanotroph-related proxies in peat deposits
683 from Misten Bog, Hautes-Fagnes, Belgium. *Org. Geochem.* **53**, 73-79.
- 684 van Winden J. F., Talbot H. M., Kip N., Reichart G. J., Pol A., McNamara N. P.,
685 Jetten M. S. M., den Camp H. and Sinninghe Damsté J. S. (2012b)
686 Bacteriohopanepolyol signatures as markers for methanotrophic bacteria in peat
687 moss. *Geochim. Cosmochim. Acta* **77**, 52-61.
- 688 Vázquez Riveiros N., Waelbroeck C., Skinner L., Duplessy J. C., McManus J. F.,
689 Kandiano E. S. and Bauch H. A. (2013) The "MIS 11 paradox" and ocean circulation:
690 Role of millennial scale events. *Earth Planet. Sci. Lett.* **371-372**, 258-268.
- 691 Versteegh G. J. M., Schefuß E., Dupont L., Marret F., Sinninghe Damsté J. S. and
692 Jansen J. H. F. (2004) Taraxerol and Rhizophora pollen as proxies for tracking past
693 mangrove ecosystems. *Geochim. Cosmochim. Acta* **68**, 411-422.
- 694 Wagner T., Kallweit W., Talbot H. M., Mollenhauer G., Boom A. and Zabel M. (2014)
695 Microbial biomarkers support organic carbon transport from methane-rich Amazon
696 wetlands to the shelf and deep sea fan during recent and glacial climate conditions.
697 *Org. Geochem.* **67**, 85-98.
- 698 Wakeham S. G., Amann R., Freeman K. H., Hopmans E. C., Jørgensen B. B.,
699 Putnam I. F., Schouten S., Sinninghe Damsté J. S., Talbot H. M. and Woebken D.
700 (2007) Microbial ecology of the stratified water column of the Black Sea as revealed
701 by a comprehensive biomarker study. *Org. Geochem.* **38**, 2070-2097.
- 702 Welander P. V., Hunter R. C., Zhang L. C., Sessions A. L., Summons R. E. and
703 Newman D. K. (2009) Hopanoids Play a Role in Membrane Integrity and pH
704 Homeostasis in *Rhodopseudomonas palustris* TIE-1. *J. Bacteriol.* **191**, 6145-6156.
- 705 Whalen S. C. (2005) Biogeochemistry of methane exchange between natural
706 wetlands and the atmosphere. *Environ. Eng. Sci.* **22**, 73-94.

- 707 Wuebbles D. J. and Hayhoe K. (2002) Atmospheric methane and global change.
708 *Earth-Sci. Rev.* **57**, 177-210.
- 709 Zabel M., Schneider R. R., Wagner T., Adegbe A. T., de Vries U. and Kolonic S.
710 (2001) Late Quaternary climate changes in central Africa as inferred from
711 terrigenous input to the Niger fan. *Quaternary Research* **56**, 207-217.
- 712 Zhao M. X., Dupont L., Eglinton G. and Teece M. (2003) n-alkane and pollen
713 reconstruction of terrestrial climate and vegetation for NW Africa over the last 160
714 kyr. *Org. Geochem.* **34**, 131-143.
- 715 Zhu C., Talbot H. M., Wagner T., Pan J. M. and Pancost R. D. (2010) Intense
716 aerobic methane oxidation in the Yangtze Estuary: A record from 35-
717 aminobacteriohopanepolyols in surface sediments. *Org. Geochem.* **41**, 1056-1059.

Table 1. List of 35-amino containing compounds identified in samples with corresponding abbreviated names, structures, and base peak (m/z) values. $[M+H]^+$

Compound name	Abbreviated name	Structure	Base peak m/z
35-aminobacteriohopane-32,33,34-triol	aminotriol	I	714
35-aminobacteriohopane-31,32,33,34-tetrol	aminotetrol	II	772
35-aminobacteriohopene-30,31,32,33,34-pentol	unsaturated aminopentol	IV/V	828
35-aminobacteriohopane-30,31,32,33,34-pentol	aminopentol	III	830
35-aminobacteriohopane-30,31,32,33,34-pentol	aminopentol isomer	III'	788

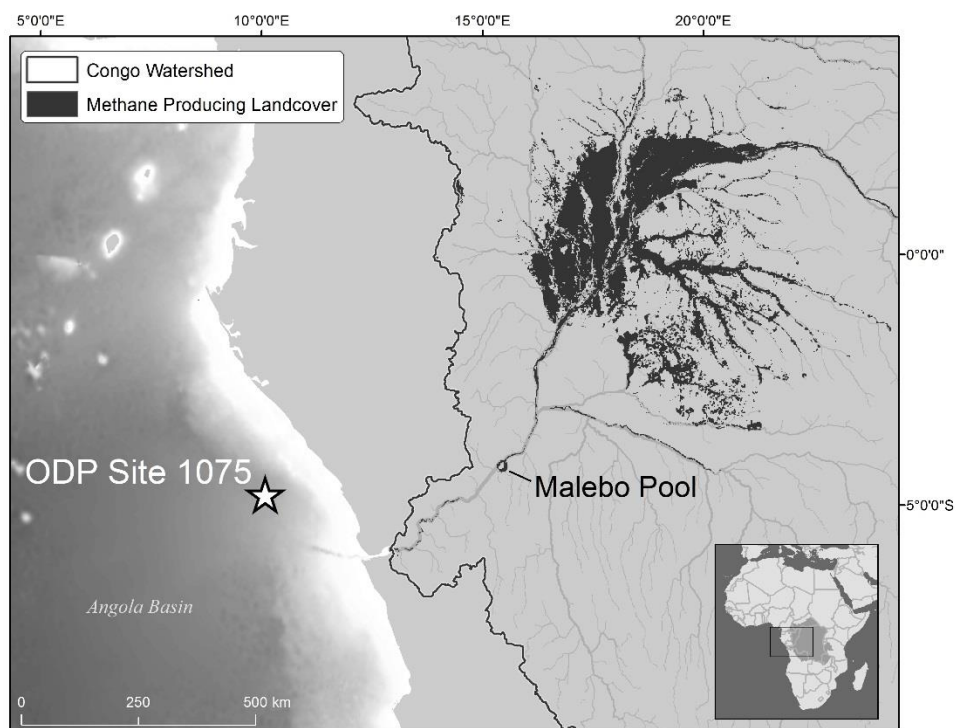


Figure 1. Map of Congo including locations of ODP 1075 and Malebo Pool.

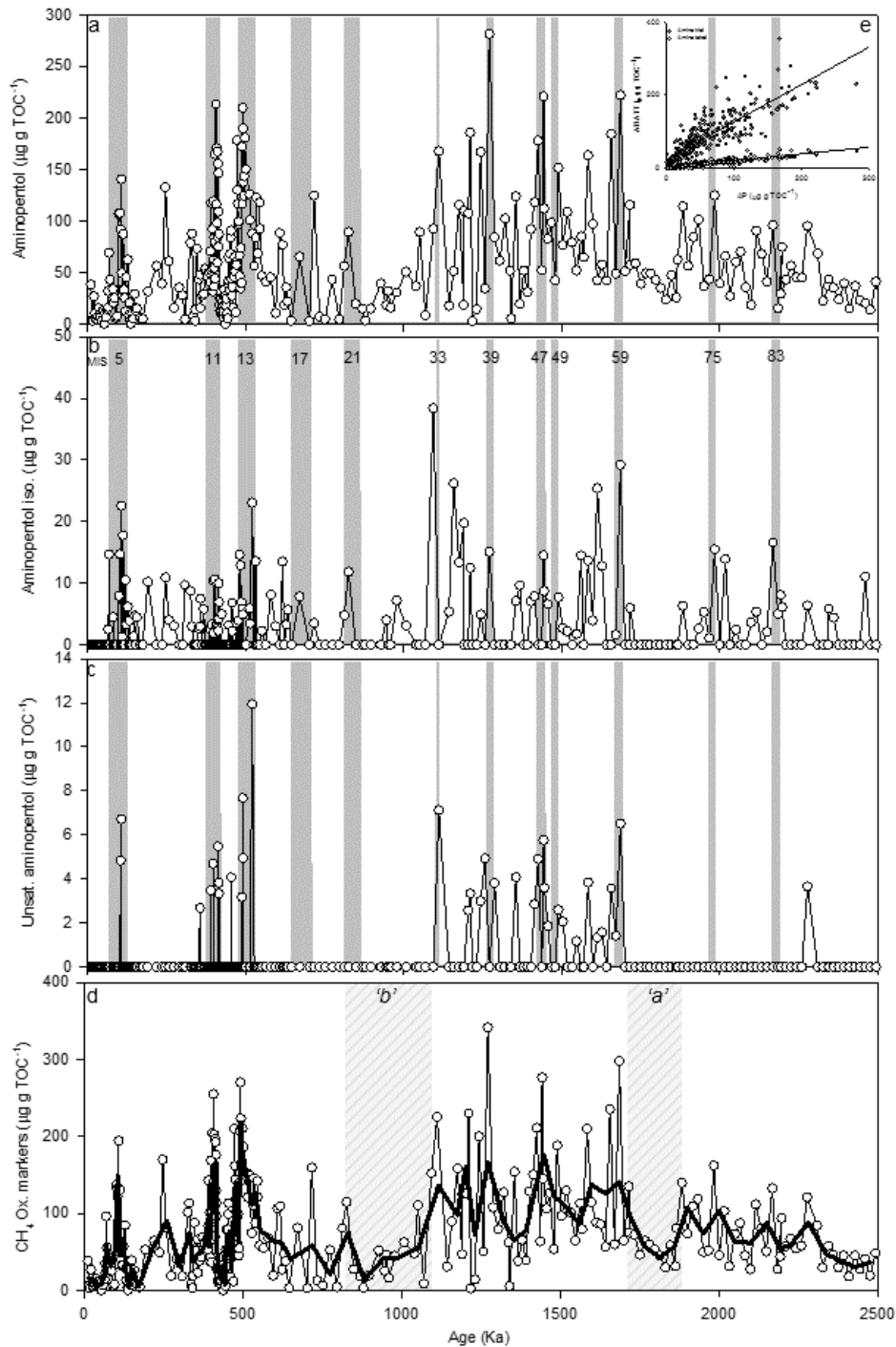


Figure 2. Concentration ($\mu\text{g gTOC}^{-1}$) of aminopentol (a), unsaturated aminopentol (b), aminopentol isomer (c), and CH_4 oxidation marker concentration (d) in ODP 1075 from 10 ka to 2.5 Ma, $\pm 20\%$ analytical error. In graph d, the black line indicates 3 point rolling average, hatched panel 'a' represents an interval from 1865-1713 ka and hatched panel 'b' represents an interval from 1099-826 ka. Correlation between aminopentol (AP) vs. aminotriol (AT) (R_s 0.891, <0.05) and aminopentol vs. aminotetrol (ATT) (R_s 0.908, $P < 0.05$) shown in e (insert). Grey bars across a, b, and c indicate selected marine isotope stages (MIS)

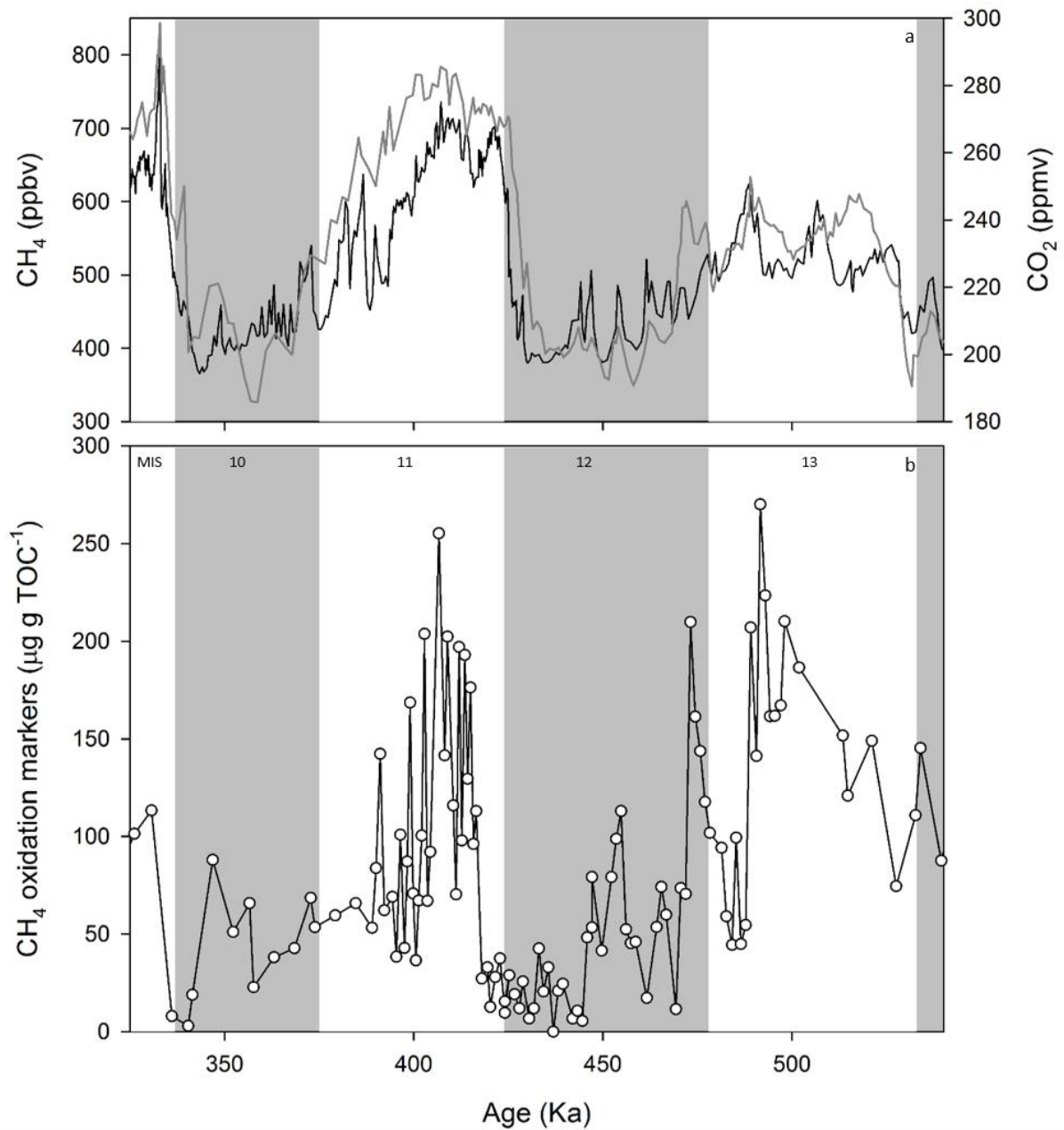


Figure 3. A; Global CH₄ (Louergue et al., 2008; Spahni et al., 2005; black, ppbv) and CO₂ concentrations (Lüthi et al., 2008; grey, ppmv). B; Concentration of CH₄ oxidation markers ($\mu\text{g gTOC}^{-1}$; ODP 1075), from 350 ka to 540 ka. Grey bars indicate MIS 10 and 12.

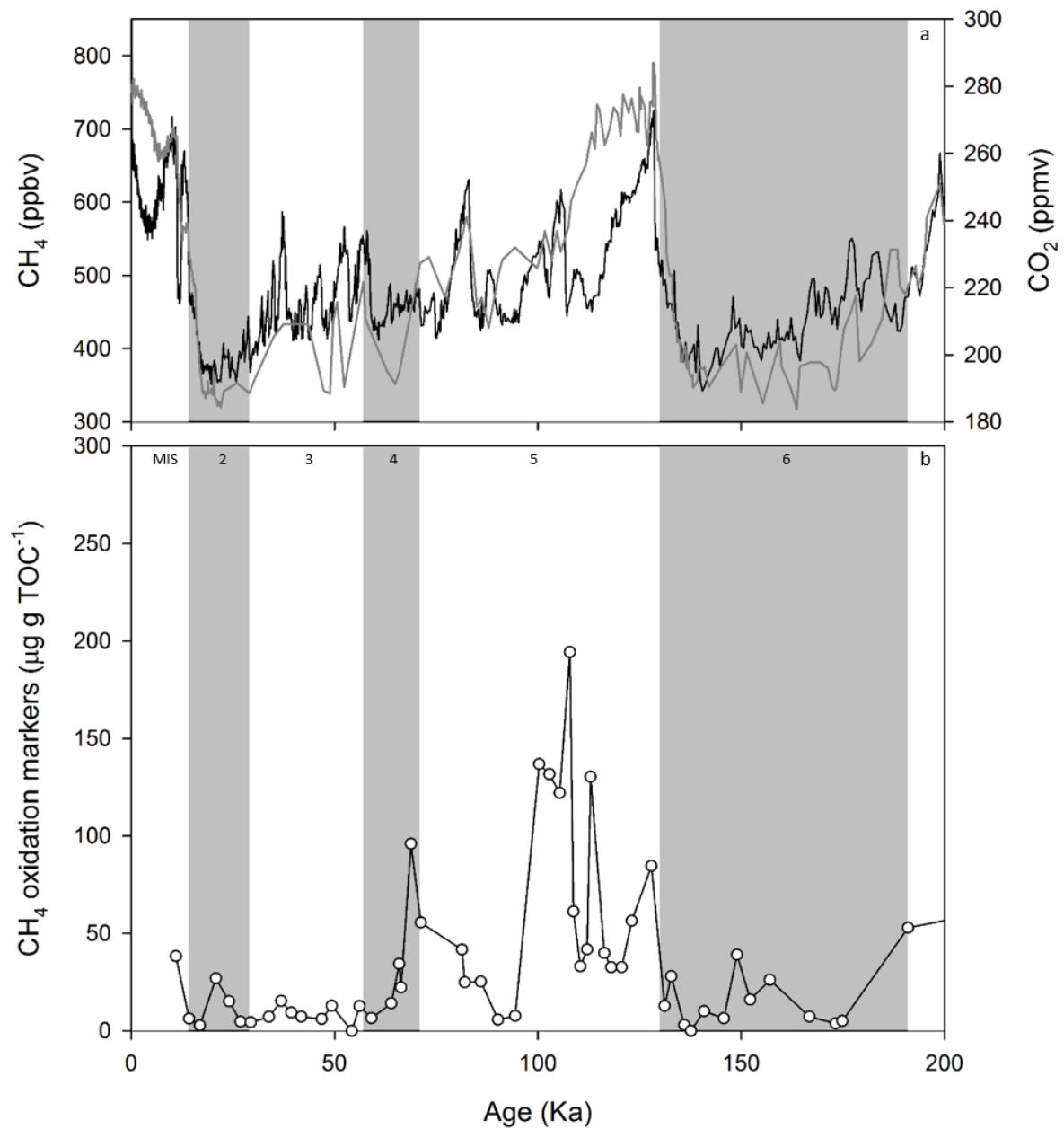


Figure 4. A; Global CH₄ (Louergue et al., 2008; Spahni et al., 2005; black, ppbv) and CO₂ concentrations (Lüthi et al., 2008; grey, ppmv). B; Concentration of CH₄ oxidation markers (µg gTOC⁻¹; ODP 1075), from 10 ka to 200 ka. Grey bars indicate MIS 2, 4 and 6.

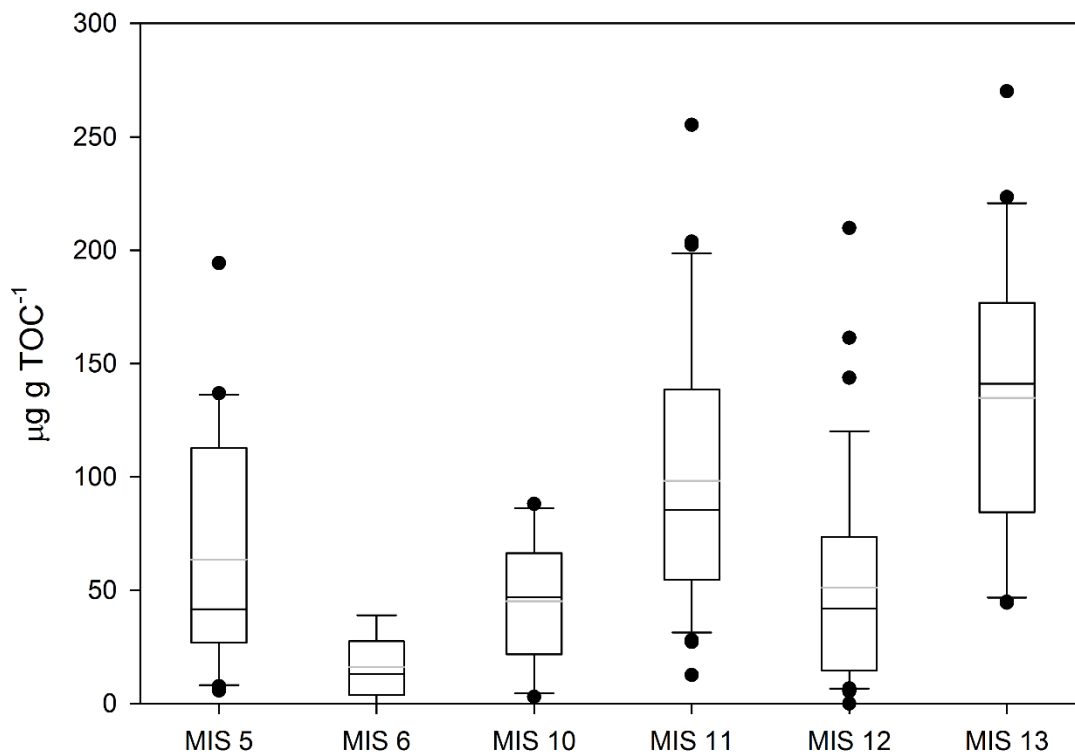


Figure 5. CH₄ oxidation marker concentration (µg gTOC⁻¹) during MIS 5 (n=20), 6 (n=8), 10 (n=10), 11 (n=36), 12 (n=38), and 13 (n=21) with median (black line) and mean (grey line) shown on each box.